IEEE Access
Multidisciplinary | Rapid Review | Open Access Journal

Received September 10, 2019, accepted September 22, 2019, date of publication September 30, 2019,
date of current version October 9, 2019.

Digital Object Identifier 10.1109/ACCESS.2019.2944406

Outage Analysis of Non-Orthogonal Multiple Access-Based Integrated Satellite-Terrestrial Relay Networks With Hardware Impairments

XIAOGANG TANG[1,3], (Member, IEEE), KANG AN[2], (Member, IEEE), KEFENG GUO[1], (Member, IEEE), YUZHEN HUANG[4], (Member, IEEE), AND SUN'AN WANG[3], (Member, IEEE)

[1]School of Space Information, Space Engineering University, Beijing 101407, China
[2]Sixty-third Research Institute, National University of Defense Technology, Nanjing 210007, China
[3]School of Mechanical Engineering, Xi'an Jiaotong University, Xi'an 710049, China
[4]Artificial Intelligence Research Center, National Innovation Institute of Defense Technology, Beijing 100039, China

Corresponding author: Kefeng Guo (guokefeng.cool@163.com)

This work was supported in part by the National Science Foundation of China under Grant 61401508, Grant 51375368, and Grant 61901502, and in part by the Research Project of National University of Defense Technology (NUDT) under Grant ZK18-02-11.

ABSTRACT In this article, we investigate the impact of hardware impairments (HIs) on the performance of non-orthogonal multiple access (NOMA) based integrated satellite-terrestrial relay networks (ISTRNs). Particularly, we obtain the novel closed-form expression for the outage probability (OP) of the considered NOMA-based ISTRNs with HIs. Furthermore, to get further insights of the effect of HIs on the considered system in high signal-to-noise ratios (SNRs) scenario, the asymptotic expression for the OP is also obtained, which provides an efficient way to evaluate the system performance, and effective quantification of different parameters on the system performance. Furthermore, we study the energy efficiency (EE) of the considered system and obtain interesting findings when NOMA scheme is applied. At last, numerical Monte Carlo (MC) results are given to verify the correctness of the theoretical results.

INDEX TERMS Non-orthogonal multiple access (NOMA), integrated satellite-terrestrial relay networks (ISTRNs), hardware impairments (HIs), outage probability (OP), energy efficiency (EE).

I. INTRODUCTION

Satellite communication (SatCom) has become a promising approach due to the growing demand for higher quality, greater capability and wider coverage of wireless services [1]. However, in practical satellite systems, the obstacles and shadowing between the satellite and the terrestrial user may result in a masking effect, which makes the line-of-sight (LOS) communication difficult to be maintained [2]. In this context, the relay cooperation is used to overcome this disadvantage, for example the fading, shadowing and path loss [3], [4]. In the era of beyond fifth-generation (5G) networks and next generation networks, the integrated satellite and terrestrial communication system has become an attractive research topic [5]–[8]. Particularly, the concept of the integrated satellite-terrestrial relay networks (ISTRNs) exploits terrestrial relays to assist the satellite signal to the destination user, which uses a terrestrial relay to aid the SatCom, has received significant attention, since it can largely increase both the reliability and throughput of wireless communication systems [9]–[11]. The authors of [9] investigated the symbol error rate (SER) of the ISTRNs with decode-and-forward (DF) protocol and interference existed, particularly, the authors obtained the closed and asymptotic expressions were also derived. In [10], the authors analyzed the performance of integrated fixed satellite service and terrestrial fixed service for Ka-band. The authors of [11] analyzed the system performance of a cognitive integrated satellite-terrestrial relay network (ISTRN) with spectrum sharing technology used, especially, the outage probability (OP) for the secondary network was derived. In [12], the authors studied the secrecy problem for the ISTRN with multiple eavesdroppers existing in the network, particularly, a new user scheduling scheme was proposed for the network. the closed-form and asymptotic expressions for the average secrecy capacity were also derived. In [13], the authors provided the approximate

The associate editor coordinating the review of this manuscript and approving it for publication was Igor Bisio.

closed-form expressions of the bit error rate (BER), OP, and capacity of the considered ISTRN, in addition, the approximated closed-form expressions for the probability density function (PDF) and cumulative distribution function (CDF) were also derived for the considered shadowed-Rician (SR) channel. In [14], the authors obtained the approximate average SER of the considered amplify-and-forward (AF) ISTRN with beamforming (BF) and combining technologies. In [15], the authors derived closed-form expressions for the OP of both primary and secondary networks with opportunistic secondary networks selection scheme. In [16], max-max relay selection scheme was applied in the considered ISTRN, where multiple terrestrial relays and multiple user were considered. Particularly, the closed-form expression for the OP of the considered ISTRN was also obtained. In [17], the novel and accurate analytical expression of the achievable ergodic capacity (EC) for the considered downlink ISTRN with multiple users and co-channel interference (CCI) was derived. In [18], the authors analyzed the secure transmission problem in the cognitive ISTRN. In [19], the authors investigated the effect of cache on the ISTRN. In [20], the authors analyzed the secure performance for the cognitive ISTRN with beamforming applied.

As mentioned before, ISTRN has been proved to be an effective approach to combat the masking effect and improve the reliability with enhanced spectrum efficiency. The other promising way to increase the spectrum efficiency for future wireless access systems is non-orthogonal multiple access (NOMA) scheme [21]. Unlike traditional orthogonal multiple access (OMA) techniques, each user in NOMA can utilize the entire available resources, e.g., time/frequenc, which results in an improved spectrum efficiency [22], [23].

Currently, only limited works have analyzed the application of NOMA scheme into ISTRN. In [24], the authors investigated the system performance, such as the EC, energy efficiency (EE), and OP of NOMA-based downlink land mobile satellite (LMS) communication networks. In [25], the authors analyzed the impact of ALOHA technology on the NOMA-based satellite communication networks. In [26], the authors focused on the cooperative transmission method in NOMA-based satellite communication networks. Besides, a joint iteration algorithm to maximize the total system capacity on the foundation of the interference temperature limit was proposed for the NOMA-based ISTRN [27]. In [28], the authors studied the exact and asymptotic expressions for the OP of the ISTRN with cooperative NOMA. In [29], the authors analyzed the EC and OP of the NOMA-based ISTRN. In [30], the authors analyzed the EC of the NOMA-based cognitive ISTRN. In [31], the authors proposed a joint BF and power allocation scheme for the NOMA-based ISTRN.

However, transmission nodes in the transmission networks are not ideal for many reasons, for example the amplifier non-linearities, in-phase/quadrature (I/Q) imbalance and phase noise [32], [33]. The authors in [34] proposed a general hardware impairments (HIs) model for the wireless relay network. In [35], the effect of HIs was analyzed for the SatCom systems, particularly, the exact and asymptotic expressions for the OP of the considered network with independent non-identical distribution (i.n.i.d) and HIs were derived. In [36], the authors investigated the impact of HIs on the two-way scenarios for the ISTRN. In [37], the authors studied the effect of HIs on the OP for the cognitive ISTRN. In [38], the authors analyzed the impacts of HIs and channel estimation errors (CEEs) on the system performance of the cognitive ISTRN. In [39], the authors investigated the impact of HIs on the uplink ISTRN with multiple terrestrial relays. To the best knowledge of the authors', the joint effects of HIs and NOMA on the ISTRN are not understood, which motivates the contributions presented in this paper.

This paper focuses on the performance of the NOMA-based ISTRN in the presence of HIs. Specifically, the main contributions of our work are summarized as follows:

- We first propose a general and practical framework for the NOMA-based ISTRN, where the promising NOMA scheme and practical HIs are considered in the network.
- Secondly, we derive the closed-form expressions for the OP and EE the NOMA-based ISTRN, which give valuable ways to evaluate the effects of the important parameters on the performance for the system.
- Lastly, we obtain the asymptotic expression for OP of the considered NOMA-based ISTRN, which provides an effective approach to quantify the system performance at high SNRs.

The remaining of this paper is shown as follows. Section II provides the system model and forms the problem of the considered NOMA-based ISTRN. Section III presents the exact closed-form expression for the OP of the considered NOMA-based ISTRN. In addition, the asymptotic analysis for the OP is also given in Section III. In Section IV, the detailed analysis for EE is derived. Numerical Monte Carlo (MC) results are obtained in Section V, which show the correctness of the theoretical analysis. Finally, our work is summarized in Section VI. The abbreviations and acronyms are presented in Table 1.

Notations: **Bold** uppercase letters present matrices and bold lowercase letters present vectors, $|\cdot|$ denotes the absolute value of a complex scalar; $\exp(\cdot)$ is the exponential function, $E[\cdot]$ is the expectation operator, $\mathcal{CN}(a, b)$ denotes the complex Gaussian distribution of a random vector a and covariance matrix b.

II. SYSTEM ILLUSTRATION AND PROBLEM FORMULATION

As shown in Figure 1, we consider a NOMA-based ISTRN which consists of a satellite (S), a terrestrial relay (R) and two destinations (namely D_1 and D_2) in this paper. DF [1] protocol is used at R. It takes two time slots for the whole transmission occurs in two time slots. In this paper, we assume that the direct link between S and D_i $i \in \{1, 2\}$ is not available for the

[1] Due to the increasing of relay's processing capacity, R can decode the signals and then forward them.

TABLE 1. Abbreviations and acronyms.

Acronym	Definition
AF	amplify-and-forward
AS	average shadowing
AWGN	additive white Gaussian noise
BF	beamforming
BER	bit error rate
CCI	co-channel interference
CDF	cumulative distribution function
CEEs	channel estimation errors
CSI	channel state information
DF	decode-and-forward
EC	ergodic capacity
EE	energy efficiency
ES	Earth station
FHS	frequency heavy shadowing
5G	fifth-generation
FSL	free space loos
GEO	geosynchronous earth orbit
GW	gateway
HIs	hardware impairments
ILS	infrequent light shadowing
i.i.d	independent identical distribution
i.n.i.d	independent non-identical distribution
I/Q	in-phase/quadrature
LMS	land mobile satellite
LOS	line-of-sight
ISTRN	integrated satellite-terrestrial relay network
ISTRNs	integrated satellite-terrestrial relay networks
MC	Monte Carlo
MRC	maximal ratio combining
NOMA	non-orthogonal multiple access
OP	outage probability
OMA	orthogonal multiple access
PA	power allocation
PDF	probability density function
SER	symbol error rate
SIC	successive interference cancelation
SINDR	signal-to-interference-plus-noise-and-distortion ratio
SNDR	signal-to-noise-and-distortion ratio
SNR	signal-to-noise ratio
SNRs	signal-to-noise ratios
SR	shadowed-Rician
TDMA	time division multiple access

reason raining, fog, or other masking effect [36]. Without loss of generality, all the transmission nodes are equipped with only one antenna, respectively.[2]

During the fist time slot, S transmits its signal $s(t)$ with $E\left[|s(t)|^2\right] = 1$ to R. The signal received at R is given by

$$y_R(t) = f_{SR,k}\left[\sqrt{P_S}s(t) + \eta_{SR}(t)\right] + n_R(t), \quad (1)$$

where $f_{SR,k}$ denotes the channel coefficient modeled as shadowed-Rician (SR) fading, P_S is the transmit power

[2]Please note that, in order to simplify the analysis, all the transmission nodes are equipped with only one antenna. However, the analysis in the following is still available for the case with multiple antennas with BF technology is applied. What's more, the derived results can be served as a benchmark of the future performance analysis and can give valuable information for the NOMA-based ISTRN.

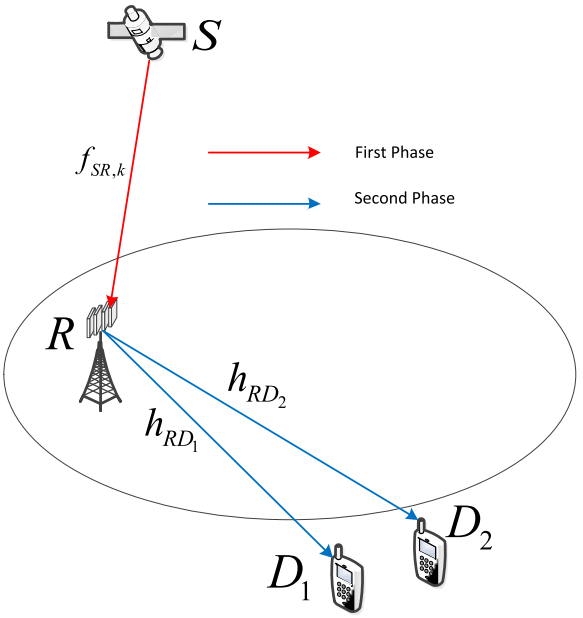

FIGURE 1. The description of the system model.

from S. On the foundation of NOMA scheme, the transmitted signal can be shown as $s(t) = a_1x_1(t) + a_2x_2(t)$, where $x_1(t)$ and $x_2(t)$ are the target transmitted signal to D_1 and D_2. Besides, we assume that $a_1 > a_2$ for the reason that the channel of user D_1 is weaker than that of user D_2; thus higher power portion is allocated to user D_1. $\eta_{SR}(t)$ is the distortion noise caused by HIs which is shown as $\eta_{SR}(t) \sim \mathcal{CN}\left(0, k_{SR_1}^2 a_1^2 P_S + k_{SR_2}^2 a_2^2 P_S\right)$[3] [35], a_1 and a_2 are the transmit power allocation (PA) factors of D_1 and D_2, respectively, according to the NOMA theme. Particularly, $a_1^2 + a_2^2 = 1$. k_{SR_1} and k_{SR_2} present the HIs level [40] for transmitted signal $x_1(t)$ and $x_2(t)$ at R, respectively, $n_R(t)$ is the additive white Gaussian noise (AWGN) at R distributed as $n_R(t) \sim \mathcal{CN}\left(0, \delta_R^2\right)$.

After R receives the signal, successive interference cancelation (SIC) is applied [21] as follows: at first, x_1 is decoded and then removed from the signal received. Then, R decodes the x_2 from the remained signal.

On this foundation, the signal-to-interference-plus-noise-and-distortion ratio (SINDR) of decoding x_1 at R can be given as

$$\gamma_{R,1} = \frac{\left|f_{SR,k}\right|^2 P_S a_1^2}{k_{SR_1}^2\left|f_{SR,k}\right|^2 P_S a_1^2 + \left|f_{SR,k}\right|^2 P_S\left(1 + k_{SR_2}^2\right)a_2^2 + \delta_R^2} = \frac{\gamma_1 a_1^2}{\gamma_1\left[k_{SR_1}^2 a_1^2 + \left(1 + k_{SR_2}^2\right)a_2^2\right] + 1}, \quad (2)$$

where $\gamma_1 = \frac{\left|f_{SR,k}\right|^2 P_S}{\delta_R^2}$.

[3]We should point out here, the HIs level not only depends on the hardware but also the transmitted signal, so here we use two different k_{SR_1} and k_{SR_2}. In the simulation Section, in order to simplify the analysis, we assume that $k_{SR_1} = k_{SR_2} = k$, which will be given detailedly in the following.

The signal-to-noise-and-distortion ratio (SNDR) of decoding x_2 at R can be given as

$$\gamma_{R,2} = \frac{\gamma_1 a_2^2}{\gamma_1 k_{SR_2}^2 a_2^2 + \gamma_1 k_{SR_1}^2 a_1^2 + 1} = \frac{\gamma_1 a_2^2}{\gamma_1 \left(k_{SR_2}^2 a_2^2 + k_{SR_1}^2 a_1^2\right) + 1}. \quad (3)$$

We should note that $\gamma_{R,2}$ can be achieved if $\gamma_{R,1} > \gamma_{th}$, i.e., the SIC is perfectly used at R to remove the signal $x_1(t)$ with γ_{th} is the outage threshold of the system.

In the second time slot, R forwards the detected superimposed signal $s(t)$ to D_1 and D_2, respectively, hence the received signal at D_i is obtained as

$$y_{D_i}(t) = h_{RD_i}\left[\sqrt{P_R}\left(\xi_1 x_1(t) + \xi_2 x_2(t)\right) + \eta_{RD}(t)\right] + n_{D_i}(t), \quad (4)$$

where h_{RD_i} is the channel coefficient between R and D_i and modeled as Rayleigh fading. P_R is the transmit power at R, $x_i(t)$ is the detected signal of the target receiver, ξ_j $j \in \{1, 2\}$ satisfying $\xi_1 > \xi_2$ and $\xi_1^2 + \xi_2^2 = 1$ are the PA factors at R, respectively.[4] $\eta_{RD}(t)$ is the distortion noise caused by HIs which is shown as $\eta_{RD}(t) \sim \mathcal{CN}\left(0, k_{RD_1}^2 \xi_1^2 P_R + k_{RD_2}^2 \xi_2^2 P_R\right)$ [35], k_{RD_1} and k_{RD_2} present the HIs level [40] for the transmitted signal at D_i, respectively, $n_{D_i}(t)$ is the AWGN at D_i distributed as $n_{D_i}(t) \sim \mathcal{CN}\left(0, \delta_{D_i}^2\right)$. Thus, D_2 implements SIC by detecting $x_1(t)$ (while considering its own message $x_2(t)$ as a noise).

With the help of (4), the SINDR at D_2 for signal $x_1(t)$ can be written as

$$\gamma_{D_2,1} = \frac{\gamma_2 \xi_1^2}{\gamma_2\left[k_{RD_1}^2 \xi_1^2 + \left(1 + k_{RD_2}^2\right)\xi_2^2\right] + 1}, \quad (5)$$

where $\gamma_2 = \frac{|h_{RD_2}|^2 P_R}{\delta_{D_2}^2}$.

With the similar restricting factor shown as (2), $\gamma_{D_2,1}$ should satisfy $\gamma_{D_2,1} \geq \gamma_{th}$. D_2 extracts the detected message from the received signal and detects its own signal, hence the final SNDR for signal $x_2(t)$ can be derived as

$$\gamma_{D_2,2} = \frac{\gamma_2 \xi_2^2}{\gamma_2\left(k_{RD_2}^2 \xi_2^2 + k_{RD_1}^2 \xi_1^2\right) + 1}. \quad (6)$$

Next, D_1 can detect $x_1(t)$ by treating $x_2(t)$ as a noise, the received SINDR at D_1 is given by

$$\gamma_{D_1,1} = \frac{\gamma_3 \xi_1^2}{\gamma_3\left[k_{RD_1}^2 \xi_1^2 + \left(1 + k_{RD_2}^2\right)\xi_2^2\right] + 1}, \quad (7)$$

where $\gamma_3 = \frac{|h_{RD_1}|^2 P_R}{\delta_{D_1}^2}$.

[4]The same channel fading is assumed here, i.e., the channel of user D_1 is weaker than that of user D_2.

As DF protocol is used at R and with the help of (2), (5) and (7), the obtained SINDR for $x_1(t)$ is given by[5]

$$\gamma_{D_1} = \min\left(\gamma_{R,1}, \gamma_{D_2,1}, \gamma_{D_1,1}\right). \quad (8)$$

Similarly, from (3) and (6), the derived SNDR at $x_2(t)$ is given by

$$\gamma_{D_2} = \min\left(\gamma_{R,2}, \gamma_{D_2,2}\right). \quad (9)$$

In this paper, we define the SINDR of the system as

$$\gamma_e = \min\left(\gamma_{D_1}, \gamma_{D2}\right) \quad (10)$$

III. PERFORMANCE ANALYSIS

In order to investigate the system performance conveniently, the statistical property of the terrestrial link and satellite links are fist obtained.

A. THE CHANNEL MODEL

1) TERRESTRIAL CHANNEL MODEL

In the considered NOMA-based system, we assume that the channel model of whole terrestrial links' is shown as independent and identically distribution (i.i.d) Rayleigh fading. On this foundation, the PDF for γ_U ($U \in \{2, 3\}$) is given by

$$f_{\gamma_U} = \frac{1}{\bar{\gamma}_U} e^{-\frac{x}{\bar{\gamma}_U}}, \quad (11)$$

where $\overline{\gamma}_U$ is the average channel gain.

The CDF of γ_U is given by

$$F_{\gamma_U} = 1 - e^{-x/\bar{\gamma}_U}. \quad (12)$$

2) SATELLITE CHANNEL MODEL

In modern satellite communications, multibeam technology is widely used to increase the spectral efficiency, which should be taken into account in modeling the satellite channel. For geosynchronous earth orbit (GEO) satellite, multiple beams are often generated through array-fed reflectors, which is more efficient than direct radiating arrays. In this case, the radiation pattern of each beam is fixed, so that the on-board precessing can be significantly reduced [41]. Furthermore, time division multiple access (TDMA) [31], [35] scheme is adopted so that there is only one Earth station (ES) scheduled within each beam at any given time.

Next, the channel coefficient $f_{SR,k}$ between the ES and the k-th on-board beam for downlink is given by

$$f_{SR,k} = C_{SR,k} h_{SR,k}, \quad (13)$$

where $h_{SR,k}$ represents the random shadowing Rician coefficient of satellite channel, and $C_{SR,k}$ denotes the radio propagation loss including the effects of free space loss (FSL) and the antenna pattern, which is described as

$$C_{SR,k} = \frac{\lambda}{4\pi} \frac{\sqrt{G_{SR,k} G_{ES}}}{\sqrt{d^2 + d_0^2}}, \quad (14)$$

[5]The signal $x_1(t)$ not only exists in R and D_1, but also exists in D_2 for the reason of NOMA scheme.

where λ denotes the carrier wavelength, d is the distance between the ES and the center of the k-th center beam, and $d_0 \approx 35786$km is the height of a GEO satellite. Besides, G_{ES} is the antenna gain of the ES and $G_{SR,k}$ is the k-th satellite on-board beam gain.

According to [42], the antenna gain for the ES with parabolic antenna can be approximately expressed as

$$G_{ES}\,(dB) \simeq \begin{cases} \overline{G}_{\max}, & for\ 0^\circ < \beta < 1^\circ \\ 32 - 25\log\beta, & for\ 1^\circ < \beta < 48^\circ \\ -10, & for\ 48^\circ < \beta \le 180^\circ, \end{cases} \tag{15}$$

where $\overline{G}_{\max}$ is the maximum beam gain at the boresight, and β denotes the off-boresight angle. As for $G_{SR,k}$, by defining θ_k as the angle between the ES position and the k-th beam center with respect to the satellite, and $\overline{\theta}_k$ as the 3dB angle of the k-th on-board beam, the antenna gain from the k-th beam to the ES is approximated by [43], [44]

$$G_{SR,k} \simeq G_{\max}\left(\frac{J_1\,(u_k)}{2u_k} + 36\frac{J_3\,(u_k)}{u_k^3}\right)^2, \tag{16}$$

where G_{max} denotes the maximal beam gain, $u_k = 2.07123\sin\theta_k/\sin\overline{\theta}_k$, J_1 and J_3 denote the first-kind bessel function of order 1 and 3, respectively. In order to get the best system performance, hence $\theta_k \to 0$,[6] as a result of $G_{SR,k} \approx G_{\max}$. On this foundation, we can have $f_{SR,k} = C_{SR,k}^{\max} h_{SR,k}$.[7]

As for the random shadowing $h_{SR,k}$, besides the mathematical models, including Loo, Barts-Stutzman, and Karasawa, the SR channel proposed in [45], is the commonly used channel model for LMS communication [9], [9], [13], [46]. According to [45], the channel coefficient $h_{SR,k}$ is modeled as $h_{SR,k} = \overline{h}_{SR,k} + \widetilde{h}_{SR,k}$, where the elements of LOS component $\overline{h}_{SR,k}$ undergo i.i.d Nakagami-m distribution while those of the scattering component $\widetilde{h}_{SR,k}$ follows the independent identical distribution (i.i.d) Rayleigh fading distribution.[8]

Furthermore, the PDF of $\gamma_1 = \bar{\gamma}_1\left|C_{SR,k}^{\max} h_{SR,k}\right|^2$ is given by

$$f_{\gamma_1}(x) = \frac{\alpha_1}{\bar{\gamma}_1} e^{-\frac{\beta_1}{\bar{\gamma}_1}}\,{}_1F_1\left(m_1; 1; \frac{\delta_1}{\bar{\gamma}_1}x\right), \quad x > 0, \tag{17}$$

where ${}_1F_1(a; b; x)$ denotes the confluent hypergeometric function defined in [52]. $\bar{\gamma}_1$ is the average signal-to-noise ratio (SNR) between the Alice and R, $\alpha_1 = \left(\frac{2b_1 m_1}{2b_1 m_1 + \Omega_1}\right)^{m_1}/2b_1$, $\beta_1 = \frac{1}{2b_1}$, $\delta_1 = \frac{\Omega_1}{2b_1(2b_1 m_1 + \Omega_1)}$ with $m_1 \ge 0$, $2b_1$, and Ω_1 are represented as the fading severity parameter ranging from 0 to ∞, the average power of the multipath component and the average power of the LOS component, respectively. In this paper, we assume that m_1 ia an integer, hence the PDF of γ_1 is given by

$$f_{\gamma_1}(x) = \alpha_1 \sum_{k_1=0}^{m_1-1} \frac{(1-m_1)_{k_1}(-\delta_1)^{k_1}}{(k_1!)^2 \bar{\gamma}_1^{k_1+1}} x^{k_1}\exp(-\Delta_1 x), \tag{18}$$

where $\Delta = \frac{\beta-\delta}{\bar{\gamma}_1}$, and $(\cdot)_k$ denotes the Pochhammer symbol [52].

On this foundation, by using [53], the CDF of γ_1 is obtained as

$$F_{\gamma_1}(x) = 1 - \alpha_1 \sum_{k_1=0}^{m_1-1}\sum_{t=0}^{k_1} \frac{(1-m_1)_{k_1}(-\delta_1)^{k_1}}{k_1!(\bar{\gamma}_1)^{k_1+1} t!\Delta_1^{k_1-t+1}} x^t e^{-\Delta_1 x}. \tag{19}$$

B. OP

From the definition of OP [37], it is defined as the SINDR falls below a predefined threshold γ_{th}, namely,

$$\begin{aligned} P_{out}(\gamma_{th}) &= \Pr(\gamma_e \le \gamma_{th}) = \Pr\left[\min\left(\gamma_{D_1}, \gamma_{D_2}\right) \le \gamma_{th}\right] \\ &= 1 - \Pr\left(\gamma_{D_1} > \gamma_{th}\right)\Pr\left(\gamma_{D_2} > \gamma_{th}\right) \\ &= P_1 + P_2 - P_1 P_2, \end{aligned} \tag{20}$$

where $P_1 = \Pr\left(\gamma_{D_1} < \gamma_{th}\right)$ and $P_2 = \Pr\left(\gamma_{D_2} < \gamma_{th}\right)$. The detailed expression for P_1 and P_2 will be given in the following.

Lemma 1: The closed-form expression for P_1 is given by

$$\begin{aligned} P_1 = 1 - \sum_{k_1=0}^{m_1-1}\sum_{i=0}^{k_1} &\frac{\alpha_1(1-m_1)_{k_1}(-\delta_1)^{k_1}}{i!\Delta_1^{k_1-i+1}\bar{\gamma}_1^{k_1+1}k_1!}\left(\frac{\Delta_1\gamma_{th}}{A - B\gamma_{th}}\right)^{k_1} \\ &\times\exp\left(-\left(\frac{\Delta_1\gamma_{th}}{A - B\gamma_{th}} + \frac{\gamma_{th}}{\bar{\gamma}_3\,(C - D\gamma_{th})} + \frac{\gamma_{th}}{\bar{\gamma}_2\,(C - D\gamma_{th})}\right)\right), \end{aligned} \tag{21}$$

where $A = a_1^2$, $B = k_{SR_1}^2 a_1^2 + \left(1 + k_{SR_2}^2\right)a_2^2$, $C = \xi_1^2$ and $D = k_{RD_1}^2\xi_1^2 + \left(1 + k_{RD_2}^2\right)\xi_2^2$.

Proof: See Appendix A. □

Lemma 2: The closed-form expression for P_2 is obtained as

$$\begin{aligned} P_2 = 1 - \sum_{k_1=0}^{m_1-1}\sum_{i=0}^{k_1} &\frac{\alpha_1(1-m_1)_{k_1}(-\delta_1)^{k_1}}{i!\Delta_1^{k_1-i+1}\bar{\gamma}_1^{k_1+1}k_1!}\left(\frac{\Delta_1\gamma_{th}}{G - H\gamma_{th}}\right)^{k_1} \\ &\times\exp\left(-\left(\frac{\Delta_1\gamma_{th}}{G - H\gamma_{th}} + \frac{\gamma_{th}}{\bar{\gamma}_2\,(P - Q\gamma_{th})}\right)\right), \end{aligned} \tag{22}$$

where $G = a_2^2$, $H = k_{SR_2}^2 a_2^2 + k_{SR_1}^2 a_1^2$, $P = \xi_2^2$ and $Q = k_{RD_2}^2\xi_2^2 + k_{RD_1}^2\xi_1^2$.

Proof: See Appendix B. □

[6] In this paper, it is noted that the location information can be available on-board the satellite, which is applicable of pointing the radiation direction to the maximum direction for the ES. Hence, here we considered the maximum case.

[7] Since satellite links are slow fading process, it is commonly assumed that the channel experiences slow fading and perfect channel state information (CSI) is available. This can be realized by feedback/ training sent from the terminals via a return channel. It is noted that here, by using software defined architecture, a gateway (GW) operates as a control center to collect and manage various kinds of information in the whole network, and the perfect CSI is available at the GW, which can be realized by feedback/training sent from the user terminals via a return channel, and has already been presented in DVB-S2 [47].

[8] The SR channel is a very popular channel model that is used in the satellite transmission links [11], [12], [15], [16]. The SR channel is a Rice model in which the LOS is random. Among the proposed models for land mobile satellite channels, the SR model proposed originally by Loo [48] has found wide applications in different frequency bands such as the UHF-band [49], L-band [50], S-band [51], and Ka-band [48]. In Loo's model, the amplitude of the LOS component is assumed to be a lognormal random variable.

C. ASYMPTOTIC OP

In the following, in order to obtain further insights of the effect of important system parameters on the OP of the considered NOMA-based ISTRN at high SNRs. Hence, we give the following analysis.

To obtain deep understanding at high SNRs, the asymptotic OP is necessary to be derived. Recalling (12) and (19), when $\overline{\gamma}_1$ is growing larger enough, they can be re-given by

$$F_{\gamma_1}(x) \approx \frac{\alpha_1}{\bar{\gamma}_1} x + o(x), \tag{23}$$

where $o(x)$ is the infinitesimal of higher order for x.

By the same way, when $\overline{\gamma}_U$ is growing larger enough, (11) is re-obtained as

$$F_{\gamma_U}(x) \approx \frac{x}{\bar{\gamma}_U} + o(x). \tag{24}$$

Lemma 3: The asymptotic expression for OP of the considered system is given by

$$P_{out}^{\infty}(\gamma_{th}) \approx \frac{\alpha_1}{\overline{\gamma}_1}\left(\frac{\gamma_{th}}{A - B\gamma_{th}} + \frac{\gamma_{th}}{G - H\gamma_{th}}\right) + \frac{\gamma_{th}}{\bar{\gamma}_3 (C - D\gamma_{th})} + \frac{\gamma_{th}}{\bar{\gamma}_2}\left[\frac{1}{(C - D\gamma_{th})} + \frac{1}{(P - Q\gamma_{th})}\right]. \tag{25}$$

Proof: By replacing (12), (19) with (24) and (23), respectively, and following the similar ways and ignoring higher order terms, (25) will be derived. □

In this sequal, we obtain the diversity order and coding gain. By letting $\bar{\gamma}_1 = \bar{\gamma}_2 = \bar{\gamma}_3 = \bar{\gamma}$, then (25) is given by

$$P_{out}^{\infty}(\gamma_{th}) \approx G_a \left(\frac{1}{\overline{\gamma}}\right)^{G_d}, \tag{26}$$

where $G_d = 1$ is the diversity order and the coding gain of the considered NOMA-based ISTRN is derived as

$$G_a = \frac{\alpha_1 \gamma_{th}}{A - B\gamma_{th}} + \frac{\alpha_1 \gamma_{th}}{G - H\gamma_{th}} + \frac{2\gamma_{th}}{C - D\gamma_{th}} + \frac{\gamma_{th}}{P - Q\gamma_{th}}. \tag{27}$$

IV. ENERGY EFFICIENCY

In ISTRNs, the satellite and the terrestrial nodes are often powered by solar panels or batteries, more reliable transmission is commonly achieved at the expense of more transmission power consumed. However, the recharge/discharge technologies have been an important issue to limit the development in ISTRNs. Hence, it is very necessary for us to investigate the EE for the considered NOMA-based ISTRNs rather than only analyzing the transmission. With the help of [54], the definition of EE is shown as

$$\theta_{EE} = \frac{R_{sys}}{\zeta P_s + P_{int}}, \tag{28}$$

where R_{sys} presents the system sum rate, $\zeta > 1$ depends on the efficiency of power amplifier, P_{int} denotes the fixed power consumption which consists the circuit power and other waste power. In this paper, we assume that $R_{sys} = C_{sys} = \log_2(1 + \gamma_e)$, hence (28) is rewritten as

$$\theta_{EE} = \frac{\log_2(1 + \gamma_e)}{\xi P_s + P_{int}}. \tag{29}$$

TABLE 2. System parameters.

Parameters	Value
Satellite Orbit	GEO
Frequency band	$f = 2$GHz
3dB angle	$\bar{\theta}_k = 0.8^\circ$
Maximal Beam Gain	$G_{max} = 48$dB
The Antenna Gain	$G_{ES} = 4$dB

TABLE 3. Channel parameters.

Shadowing	m_1	b_1	Ω_1
Frequent heavy shadowing (FHS)	1	0.063	0.0007
Average shadowing (AS)	5	0.251	0.279
Infrequent light shadowing (ILS)	10	0.158	1.29

V. NUMERICAL RESULTS

In this section, MC results are given to verify the correctness of the performance analysis. With losing of no generality, we set $\delta_R^2 = \delta_{D_1}^2 = \delta_{D_2}^2 = 1$ and denote $\overline{\gamma}_1 = \overline{\gamma}_2 = \overline{\gamma}_3 = \overline{\gamma}$, $k_{SR_1} = k_{SR_2} = k_{RD_1} = k_{RD_2} = k$. Besides, we consider γ_{th}=3dB for the OP analysis in Figure 2, Figure 3 and Figure 5. The system and channel parameters are given in Table 2 [39] and Table 3 [53], respectively. Different power coefficient combinations, namely, Case I: $a_1^2 = \xi_1^2 = 0.7$, $a_2^2 = \xi_2^2 = 0.3$; Case II: $a_1^2 = \xi_1^2 = 0.8$, $a_2^2 = \xi_2^2 = 0.2$ are adopted. In Figure 4, we set $\overline{\gamma} = 30$dB. $\zeta = 2$, $P_{int} = 5dBW$ [23] for Figure 6 and Figure 7.

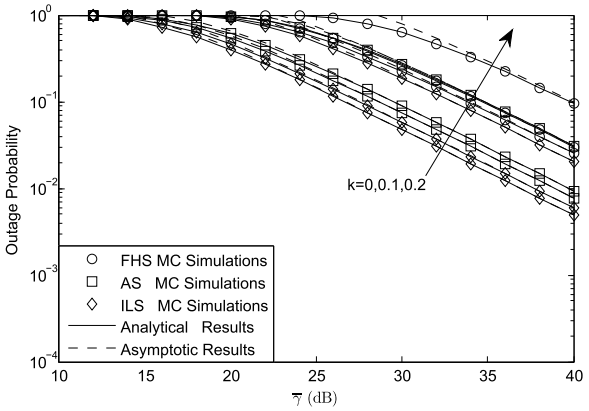

FIGURE 2. OP versus $\bar{\gamma}$ with Case I.

Figures 2-5 depict the OP of the considered NOMA-based system. We can find that the analytical results are the same with the MC simulations. The asymptotic results are tight across the simulations at high SNRs, which confirm the correctness of our theoretical results. Moreover, we can find

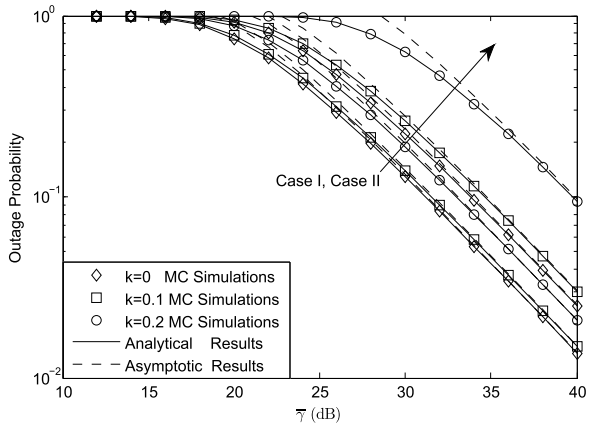

FIGURE 3. OP versus $\bar{\gamma}$ between Case I and Case II, respectively, for FHS.

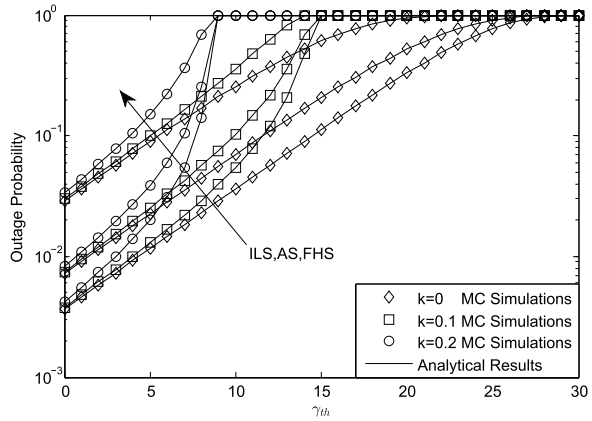

FIGURE 4. OP versus different γ_{th} for Case I.

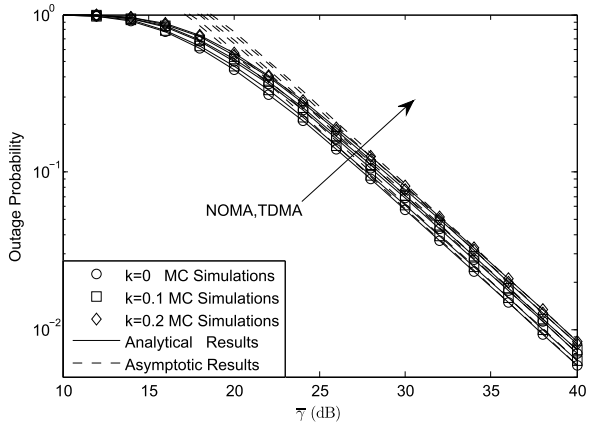

FIGURE 5. OP versus $\bar{\gamma}$ for Case I of x_2 between NOMA and TDMA [31], [35].

that from the comparison between Figure 2 and Figure 3, when the power of the weak channel is larger, the OP will be enhanced. This is because the weak channel can decode the signal easily. In addition, we can observe that the SINDR would have an upper bound in Figure 4, namely, when γ_{th} is larger than a specific value, the OP would be always one as γ_{th} grows to infinity. Moreover, we find that the system has the same specific value for different channel fading, which means that this specific value is the function of HIs' level, not the function of channel fading. Finally, from Figure 5, we show that the OP of NOMA system is lower than that of TDMA, which confirms the advantage of employing NOMA scheme.

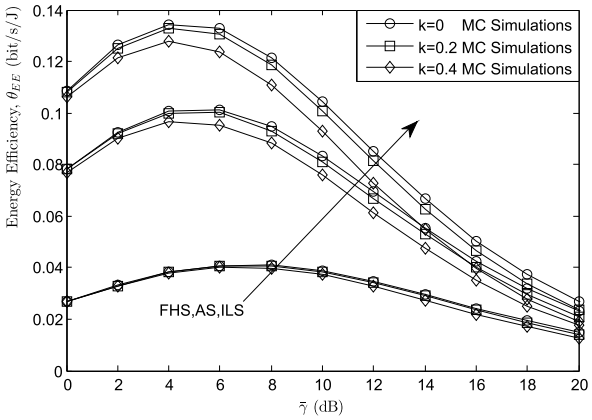

FIGURE 6. The energy efficiency of the considered system versus $\bar{\gamma}$ for different channel fading and HIs levels.

Figure 6 examines the energy efficiency of the considered system versus $\bar{\gamma}$ for different channel fading and HIs' levels. From Figure 6, we can observe that the EE will be larger when the level of HIs is smaller. Besides, we can find that the EE will be enhanced when the channel suffers heavy fading. We also can find that at first, the EE curves significantly increase and then, after a certain value, EE decrease with $\bar{\gamma}$ increasing. It is very interesting that, the specific value take place at a small $\bar{\gamma}$.

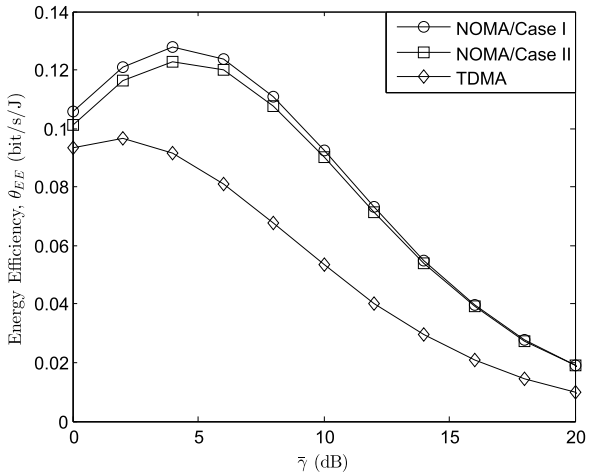

FIGURE 7. The energy efficiency of the considered system between NOMA and TDMA versus $\bar{\gamma}$ for ILS with $k = 0.2$.

Figure 7 shows the EE of the considered system between NOMA and TDMA [31], [35] versus $\bar{\gamma}$ for ILS with $k = 0.2$. At the same time, it can be found that the EE curves

of the NOMA scheme are superior to that of the TDMA scheme, since higher capacity can be achieved with the same amount of power consumption. This observation shows that when NOMA scheme is applied in the considered ISTRN, the energy consumption is significantly alleviated, which is very useful and helpful for the case with limited energy resources, namely, solar panel, battery pack. In addition, it can further give a good industrial suggestion, for the reason that smaller rockets will be selected.

VI. CONCLUSION

In this paper, we investigated the effects of HIs on the performance of NOMA-based ISTRNs. Particularly, we derived the closed-form expression for the OP of the considered NOMA-based ISTRNs. In order to obtain deep insights, we provided the asymptotic expression for OP in high SNR regime. Moreover, the diversity order and coding gain were also derived. The obtained results provided efficient ways to evaluate the impact of HIs on the performance of the considered ISTRNs. Furthermore, we analyzed the EE of the system and found that there existed a maximum value for the energy efficiency of the system when NOMA scheme was applied. Furthermore, the system performance can be obviously improved under the light shadowing, while significantly degraded when the level of the HIs was larger.

APPENDIX A
PROOF OF LEMMA 1

Recalling (20), P_1 can be rewritten as

$$\begin{aligned}
&P_1\\
&= \Pr\left(\gamma_{D_1} \le \gamma_{th}\right) = \Pr\left(\min\left(\gamma_{R,1}, \gamma_{D_2,1}, \gamma_{D_1,1}\right) \le \gamma_{th}\right)\\
&= \Pr\left\{\min\left[\gamma_{R,1}, \min\left(\gamma_{D_2,1}, \gamma_{D_1,1}\right)\right] \le \gamma_{th}\right\}\\
&= \Pr\left(\gamma_{R,1} \le \gamma_{th}\right)\left[1- \Pr\left(\gamma_{D_2,1} \le \gamma_{th}\right) - \Pr\left(\gamma_{D_1,1} \le \gamma_{th}\right)\right.\\
&\quad \left. + \Pr\left(\gamma_{D_2,1} \le \gamma_{th}\right)\Pr\left(\gamma_{D_1,1} \le \gamma_{th}\right)\right] + \left[\Pr\left(\gamma_{D_2,1} \le \gamma_{th}\right)\right.\\
&\quad \left. + \Pr\left(\gamma_{D_1,1} \le \gamma_{th}\right) - \Pr\left(\gamma_{D_2,1} \le \gamma_{th}\right)\Pr\left(\gamma_{D_1,1} \le \gamma_{th}\right)\right].
\end{aligned} \tag{30}$$

With the help of (2), $\Pr\left(\gamma_{R,1} \le \gamma_{th}\right)$ can be given by

$$\Pr\left(\gamma_{R,1} \le \gamma_{th}\right) = F_{\gamma_1}\left(\gamma_{th}/\left(A - B\gamma_{th}\right)\right). \tag{31}$$

With the help of (19), (31) can be rewritten as

$$\begin{aligned}
&\Pr\left(\gamma_{R,1} \le \gamma_{th}\right)\\
&= 1 - \alpha_1 \sum_{k_1=0}^{m_1-1}\sum_{t=0}^{k_1} \frac{(1-m_1)_{k_1}(-\delta_1)^{k_1}\gamma_{th}^{t} e^{-\Delta_1\gamma_{th}/(A-B\gamma_{th})}}{k_1!(\bar{\gamma}_1)^{k_1+1}t!\Delta_1^{k_1-t+1}(A-B\gamma_{th})^{t}}.
\end{aligned} \tag{32}$$

Utilizing the similar approaches, $\Pr\left(\gamma_{D_2,1} \le \gamma_{th}\right)$ and $\Pr\left(\gamma_{D_1,1} \le \gamma_{th}\right)$ can be obtained as

$$\Pr\left(\gamma_{D_2,1} \le \gamma_{th}\right) = F_{\gamma_2}\left(\gamma_{th}/\left(C - D\gamma_{th}\right)\right), \tag{33a}$$

$$\Pr\left(\gamma_{D_1,1} \le \gamma_{th}\right) = F_{\gamma_3}\left(\gamma_{th}/\left(C - D\gamma_{th}\right)\right). \tag{33b}$$

Then with the help of (12), (33a) and (33b) are given by

$$\Pr\left(\gamma_{D_2,1} \le \gamma_{th}\right) = 1 - \exp\left(\gamma_{th}/\left(C - D\gamma_{th}\right)/\overline{\gamma}_2\right), \tag{34a}$$

$$\Pr\left(\gamma_{D_1,1} \le \gamma_{th}\right) = 1 - \exp\left(\gamma_{th}/\left(C - D\gamma_{th}\right)/\overline{\gamma}_3\right). \tag{34b}$$

By substituting (32), (34a) and (34b) into (30), and after necessary mathematical calculations, the closed-form expression for P_1 will be eventually obtained.

The proof is completed.

APPENDIX B
PROOF OF LEMMA 2

Again from (9), P_2 can be rewritten as

$$\begin{aligned}
P_2 = \Pr\left(\gamma_{D_2} \le \gamma_{th}\right) &= \left[\Pr\left(\gamma_{D_2,2} \le \gamma_{th}\right)\right.\\
&\quad \left. + \Pr\left(\gamma_{R,2} \le \gamma_{th}\right) - \Pr\left(\gamma_{D_2,2} \le \gamma_{th}\right)\Pr\left(\gamma_{R,2} \le \gamma_{th}\right)\right].
\end{aligned} \tag{35}$$

Then with the similar ways as Appendix A, we can get

$$\begin{aligned}
&\Pr\left(\gamma_{R,2} \le \gamma_{th}\right)\\
&= F_{\gamma_1}\left(\gamma_{th}/\left(G - H\gamma_{th}\right)\right)\\
&= 1 - \alpha_1 \sum_{k_1=0}^{m_1-1}\sum_{t=0}^{k_1} \frac{(1-m_1)_{k_1}(-\delta_1)^{k_1}\gamma_{th}^{t} e^{-\Delta_1\gamma_{th}/(G-H\gamma_{th})}}{k_1!(\bar{\gamma}_1)^{k_1+1}t!\Delta_1^{k_1-t+1}(G-H\gamma_{th})^{t}},
\end{aligned} \tag{36a}$$

$$\begin{aligned}
&\Pr\left(\gamma_{D_2,2} \le \gamma_{th}\right)\\
&= F_{\gamma_2}\left(\gamma_{th}/\left(P - Q\gamma_{th}\right)\right)\\
&= 1 - \exp\left(\gamma_{th}/\left(P - Q\gamma_{th}\right)/\overline{\gamma}_2\right).
\end{aligned} \tag{36b}$$

Then, by utilizing (36a) and (36b) into (35), the final closed-form expression for P_2 will be derived.

The proof is completed.

REFERENCES

[1] D. Tse and P. Viswanath, *Fundamentals of Wireless Communication*. Cambridge, U.K.: Cambridge Univ. Press, 2005.

[2] B. Evans, M. Werner, E. Lutz, M. Bousquet, G. E. Corazza, G. Maral, and R. Rumeau, "Integration of satellite and terrestrial systems in future multimedia communications," *IEEE Wireless Commun.*, vol. 12, no. 5, pp. 72–80, Oct. 2005.

[3] J. N. Laneman, D. N. C. Tse, and G. W. Wornell, "Cooperative diversity in wireless networks: Efficient protocols and outage behavior," *IEEE Trans. Inf. Theory*, vol. 50, no. 12, pp. 3062–3080, Dec. 2004.

[4] M. Li, M. Lin, Q. Yu, W.-P. Zhu, and L. Dong, "Optimal beamformer design for dual-hop MIMO AF relay networks over Rayleigh fading channels," *IEEE J. Sel. Areas Commun.*, vol. 30, no. 8, pp. 1402–1414, Sep. 2012.

[5] P. Chini, G. Giambene, and S. Kota, "A survey on mobile satellite systems," *Int. J. Satelite Commun.*, vol. 28, no. 1, pp. 29–57, Aug. 2009.

[6] K. An, M. Lin, T. Liang, J.-B. Wang, J. Wang, Y. Huang, and A. L. Swindlehurst, "Performance analysis of multi-antenna hybrid satellite-terrestrial relay networks in the presence of interference," *IEEE Trans. Commun.*, vol. 63, no. 11, pp. 4390–4404, Nov. 2015.

[7] G. Araniti, I. Bisio, M. De Sanctis, A. Orsino, and J. Cosmas, "Multimedia content delivery for emerging 5G-satellite networks," *IEEE Trans. Broadcast.*, vol. 3, no. 1, pp. 10–23, Mar. 2016.

[8] M. de Sanctis, E. Cianca, G. Araniti, I. Bisio, and R. Prasad, "Satellite communications supporting Internet of remote things," *IEEE Internet Things J.*, vol. 3, no. 1, pp. 113–123, Feb. 2016.

[9] M. R. Bhatnagar and M. K. Arti, "Performance analysis of AF based hybrid satellite-terrestrial cooperative network over generalized fading channels," *IEEE Commun. Lett.*, vol. 17, no. 10, pp. 1912–1915, Oct. 2013.

[10] K. An, T. Liang, G. Zheng, X. Yan, Y. Li, and S. Chatzinotas, "Performance limits of cognitive uplink FSS and terrestrial FS for Ka-band," *IEEE Trans. Aerosp. Electron. Syst.*, to be published.

[11] K. An, M. Lin, W.-P. Zhu, Y. Huang, and G. Zheng, "Outage performance of cognitive hybrid satellite–terrestrial networks with interference constraint," *IEEE Trans. Veh. Technol.*, vol. 65, no. 11, pp. 9397–9404, Nov. 2016.

[12] K. Guo, K. An, B. Zhang, Y. Huang, and D. Guo, "Physical layer security for hybrid satellite terrestrial relay networks with joint relay selection and user scheduling," *IEEE Access*, vol. 6, pp. 55815–55827, 2018.

[13] R. B. Manav and M. K. Arti, "On the closed-form performance analysis of maximal ratio combining in shadowed-rician fading LMS channels," *IEEE Commun. Lett.*, vol. 18, no. 1, pp. 54–57, Jan. 2014.

[14] M. K. Arti and M. R. Bhatnagar, "Beamforming and combining in hybrid satellite-terrestrial cooperative systems," *IEEE Commun. Lett.*, vol. 18, no. 3, pp. 483–486, Mar. 2014.

[15] P. K. Sharma, P. K. Upadhyay, D. B. da Costa, P. S. Bithas, and A. G. Kanatas, "Performance analysis of overlay spectrum sharing in hybrid satellite-terrestrial systems with secondary network selection," *IEEE Trans. Wireless Commun.*, vol. 16, no. 10, pp. 6586–6601, Oct. 2017.

[16] P. K. Upadhyay and P. K. Sharma, "Max-max user-relay selection scheme in multiuser and multirelay hybrid satellite-terrestrial relay systems," *IEEE Commun. Lett.*, vol. 20, no. 2, pp. 268–271, Feb. 2016.

[17] V. Bankey and P. K. Upadhyay, "Ergodic capacity of multiuser hybrid satellite-terrestrial fixed-gain AF relay networks with CCI and outdated CSI," *IEEE Trans. Veh. Technol.*, vol. 67, no. 5, pp. 4666–4671, May 2018.

[18] B. Li, Z. Fei, Z. Chu, F. Zhou, K.-K. Wong, and P. Xiao, "Robust chance-constrained secure transmission for cognitive satellite–terrestrial networks," *IEEE Trans. Veh. Technol.*, vol. 67, no. 5, pp. 4208–4219, May 2018.

[19] K. An, Y. Li, X. Yan, and T. Liang, "On the performance of cache-enabled hybrid satellite-terrestrial relay networks," *IEEE Wireless Commun. Lett.*, to be published.

[20] K. An , M. Lin, J. Ouyang, and W.-P. Zhu, "Secure transmission in cognitive satellite terrestrial networks," *IEEE J. Sel. Areas Commun.*, vol. 34, no. 11, pp. 3025–3037, Nov. 2016.

[21] S. Arzykulov, T. A. Tsiftsis, G. Nauryzbayev, M. Abdallah, and G. Yang, "Outage performance of underlay CR-NOMA networks with detect-and-forward relaying," in *Proc. IEEE Globecom*, Abu Dhabi, United Arab Emirates, Dec. 2018, pp. 1–6.

[22] S. M. R. Islam, M. Zeng, O. A. Dobre, and K.-S. Kwak, "Resource allocation for downlink NOMA systems: Key techniques and open issues," *IEEE Wireless Commun.*, vol. 25, no. 2, pp. 40–47, Apr. 2018.

[23] X. Tang, K. An, K. Guo, S. Wang, X. Wang, J. Li, and F. Zhou, "On the performance of two-way multiple relay non-orthogonal multiple access-based networks with hardware impairments," *IEEE Access*, vol. 7, pp. 128896–128909, Sep. 2019. doi: 10.1109/ACCESS.2019.2939436.

[24] X. Yan, H. Xiao, C.-X. Wang, K. An, A. T. Chronopoulos, and G. Zheng, "Performance analysis of NOMA-Based land mobile satellite networks," *IEEE Access*, vol. 6, pp. 31327–31339, 2018.

[25] X. Shao, Z. Sun, M. Yang, S. Gu, and Q. Guo, "NOMA-based irregular repetition slotted ALOHA for satellite networks," *IEEE Commun. Lett.*, vol. 23, no. 4, pp. 624–627, Apr. 2019.

[26] R. Wan, L. Zhu, T. Li, and L. Bai, "A NOMA-PSO based cooperative transmission method in satellite communication systems," in *Proc. IEEE WCSP*, Nanjing, China, Oct. 2017, pp. 1–6.

[27] X. Zhu, C. Jiang, L. Kuang, N. Ge, and J. Lu, "Non-orthogonal multiple access based integrated terrestrial-satellite networks," *IEEE J. Sel. Areas Commun.*, vol. 35, no. 10, pp. 2253–2267, Oct. 2017.

[28] X. Yan, H. Xiao, C.-X. Wang, and K. An, "Outage performance of NOMA-based hybrid satellite-terrestrial relay networks," *IEEE Wireless Commun. Lett.*, vol. 7, no. 4, pp. 538–541, Aug. 2018.

[29] X. Yan, H. Xiao, K. An, G. Zheng, and W. Tao, "Hybrid satellite terrestrial relay networks with cooperative non-orthogonal multiple access," *IEEE Commun. Lett.*, vol. 22, no. 5, pp. 978–981, May 2018.

[30] X. Yan, H. Xiao, K. An, G. Zheng, and S. Chatzinotas, "Ergodic capacity of NOMA-based uplink satellite networks with randomly deployed users," *IEEE Syst. J.*, to be published. doi: 10.1109/JSYST.2019.2934358.

[31] Z. Lin, M. Lin, J.-B. Wang, T. de Cola, and J. Wang, "Joint beamforming and power allocation for satellite-terrestrial integrated networks with non-orthogonal multiple access," *IEEE J. Sel. Areas Commun.*, vol. 13, no. 3, pp. 657–670, Jun. 2019.

[32] E. Costa and S. Pupolin, "M-QAM-OFDM system performance in the presence of a nonlinear amplifier and phase noise," *IEEE Trans. Commun.*, vol. 50, no. 3, pp. 462–472, Mar. 2002.

[33] X. Zhang, D. Guo, K. An, and B. Zhang, "Secure communications over cell-free massive MIMO networks with hardware impairments," *IEEE Syst. J.*, to be published. doi: 10.1109/JSYST.2019.2919584.

[34] E. Bjornson, M. Matthaiou, and M. Debbah, "A new look at dual-hop relaying: Performance limits with hardware impairments," *IEEE Trans. Commun.*, vol. 61, no. 11, pp. 4512–4525, Nov. 2013.

[35] K. Guo, M. Lin, B. Zhang, W.-P. Zhu, J.-B. Wang, and T. A. Tsiftsis, "On the performance of LMS communication with hardware impairments and interference," *IEEE Trans. Commun.*, vol. 67, no. 2, pp. 1490–1505, Feb. 2019.

[36] K. Guo, B. Zhang, Y. Huang, and D. Guo, "Performance analysis of two-way satellite terrestrial relay networks with hardware impairments," *IEEE Wireless Commun. Lett.*, vol. 6, no. 4, pp. 430–433, Aug. 2017.

[37] K. Guo, K. An, B. Zhang, Y. Huang, and G. Zheng, "Outage analysis of cognitive hybrid satellite-terrestrial networks with hardware impairments and multi-primary users," *IEEE Wireless Commun. Lett.*, vol. 7, no. 5, pp. 816–819, Oct. 2018.

[38] K. Guo, K. An, B. Zhang, Y. Huang, and D. Guo, "On the performance of cognitive satellite-terrestrial relay networks with channel estimation error and hardware impairments," *Sensors*, vol. 18, no. 10, p. 3292, Sep. 2018.

[39] K. Guo, K. An, B. Zhang, Y. Huang, D. Guo, G. Zheng, and S. Chatzinotas, "On the performance of the uplink satellite multiterrestrial relay networks with hardware impairments and interference," *IEEE Syst. J.*, vol. 13, no. 3, pp. 2297–2308, Sep. 2019.

[40] "8 hints for making and interpreting EVM measurements," Agilent Technologies, Santa Clara, CA, USA, Tech. Rep. 5989-3144EN, 2005.

[41] J. Arnau, D. Christopoulos, S. Chatzinotas, C. Mosquera, and B. Ottersten, "Performance of the multibeam satellite return link with correlated rain attenuation," *IEEE Trans. Wireless Commun.*, vol. 13, no. 11, pp. 6286–6299, Nov. 2014.

[42] *Prediction Procedure for the Evaluation of Interference Between Stations on the Surface of the Earth At Frequencies Above About 0.1 GHz*, document ITU-R P.452, Sep. 2013.

[43] W. Lu, K. An, and T. Liang, "Robust beamforming design for sum secrecy rate maximization in multibeam satellite systems," *IEEE Trans. Aerosp. Electron. Syst.*, vol. 55, no. 3, pp. 1568–1572, Jun. 2019.

[44] K. An, T. Liang, X. Yan, and G. Zheng, "On the secrecy performance of land mobile satellite communication systems," *IEEE Access*, vol. 6, pp. 39606–39620, 2018.

[45] A. Abdi, W. C. Lau, M.-S. Alouini, and M. Kaveh, "A new simple model for land mobile satellite channels: First- and second-order statistics," *IEEE Trans. Wireless Commun.*, vol. 2, no. 3, pp. 519–528, May 2003.

[46] M. K. Arti and K. J. Suresh, "OSTBC transmission in shadowed-rician land mobile satellite links," *IEEE Trans. Veh. Technol.*, vol. 65, no. 7, pp. 5771–5777, Jul. 2016.

[47] A. Morello and V. Mignone, "DVB-S2: The second generation standard for satellite broad-band services," *Proc. IEEE*, vol. 94, no. 1, pp. 210–227, Jan. 2006.

[48] C. Loo, "A statistical model for a land mobile satellite link," *IEEE Trans. Veh. Technol.*, vol. VT-34, no. 3, pp. 122–127, Aug. 1985.

[49] C. Loo and J. S. Butterworth, "Land mobile satellite channel measurements and modeling," *Proc. IEEE*, vol. 86, no. 7, pp. 1442–1463, Jul. 1998.

[50] B. Vucetic and J. Du, "Channel modeling and simulation in satellite mobile communication systems," *IEEE J. Sel. Areas Commun.*, vol. 10, no. 8, pp. 1209–1218, Oct. 1992.

[51] F. Perez-Fontan, M. A. Vazquez-Castro, S. Buonomo, J. P. Poiares-Baptista, and B. Arbesser-Rastburg, "S-band LMS propagation channel behaviour for different environments, degrees of shadowing and elevation angles," *IEEE Trans. Broadcast.*, vol. 44, no. 1, pp. 40–76, Mar. 1998.

[52] I. S. Gradshteyn, I. M. Ryzhik, A. Jeffrey, and D. Zwillinger, *Table of Integrals, Series, and Products*, 7th ed. Amsterdam, The Netherlands: Elsevier, 2007.

[53] N. I. Miridakis, D. D. Vergados, and A. Michalas, "Dual-hop communication over a satellite relay and shadowed Rician channels," *IEEE Trans. Veh. Technol.*, vol. 64, no. 9, pp. 4031–4040, Sep. 2015.

[54] P. Patcharamaneepakorn, S. Wu, C.-X. Wang, E.-H. M. Aggoune, M. M. Alwakeel, X. Ge, and M. Di Renzo, "Spectral, energy, and economic efficiency of 5G multicell massive MIMO systems with generalized spatial modulation," *IEEE Trans. Veh. Technol.*, vol. 65, no. 12, pp. 9715–9731, Dec. 2016.

XIAOGANG TANG received the M.S. degree from Xi'an Jiaotong University, Shann'xi, Xi'an, China, in 2002. He is currently pursuing the Ph.D. degree with Xi'an Jiaotong University, and also an Assistant Professor of Xi'an Jiaotong University and Space Engineering University. His research interests include mechatronics, pattern recognition, signal processing, and satellite communication. He has published several research articles in scholarly journals in the above research areas and has participated in several conferences.

KANG AN received the B.S. degree from the Nanjing University of Aeronautics and Astronautics, Nanjing, China, in 2011, the M.S. degree from the PLA University of Science and Technology, Nanjing, and the Ph.D. degree from the Army Engineering University of PLA, in 2017. He is currently an Engineer with the Sixty-third Research Institute, National University of Defense Technology, Nanjing. His research interests include cooperative communication, satellite communication, cognitive radio, and physical layer security.

KEFENG GUO received the B.S. degree from the Beijing Institute of Technology, Beijing, China, in 2012, the M.S. degree from the PLA University of Science and Technology, Nanjing, China, in 2015, and the Ph.D. degree from the Army Engineering University of PLA, in 2018. He is currently a Lecturer with the School of Space Information, Space Engineering University. His research interests include cooperative relay networks, MIMO communications systems, multiuser communication systems, satellite communication, hardware impairments, cognitive radio, and physical layer security. Dr. Guo has been the TPC Member of many IEEE sponsored conferences, such as the IEEE ICC and the IEEE GLOBECOM.

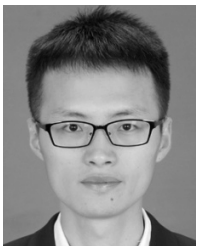

YUZHEN HUANG received the B.S. degree in communications engineering and the Ph.D. degree in communications and information systems from the College of Communications Engineering, PLA University of Science and Technology, in 2008 and 2013, respectively. He has been with the Artificial Intelligence Research Center, National Innovation Institute of Defense Technology, where he is currently an Associate Professor. He is also a Postdoctoral Research Associate with the School of Information and Communication, Beijing University of Posts and Telecommunications, Beijing. He has authored or coauthored nearly 90 research articles in international journals and conferences. His research interests include channel coding, MIMO communications systems, cooperative communications, physical layer security, and cognitive radio systems. He and his coauthors have been awarded the Best Paper Award at the WCSP 2013. He received the IEEE COMMUNICATIONS LETTERS Exemplary Reviewer Certificate, in 2014. He also serves as an Associate Editor for the *KSII Transactions on Internet and Information Systems*.

SUN'AN WANG received the Ph.D. degree from Xi'an Jiaotong University, Xi'an, Shann'xi, China, in 1989, where he is currently a Professor. He has published several research articles in scholarly journals in the above research areas and has participated in several conferences. His research interests include mechatronics, pattern recognition, satellite communication, and physical layer security.